Detailed Consideration of Experimental Results of Gyrotron FU CW II Developed as a Radiation Source for DNP-NMR Spectroscopy

**La Agusu · T. Idehara · I. Ogawa · T. Saito ·
T. Kanemaki · H. Takahashi · T. Fujiwara**

Abstract A CW gyrotron for the sensitivity enhancement of NMR spectroscopy through dynamic nuclear polarization has been designed. The gyrotron operates at the second harmonic and frequency of 394.6 GHz with the main operating mode $TE_{0,6}$. Operating conditions of other neighboring cavity modes such as $TE_{2,6}$ at frequency of 392.6 GHz and $TE_{2,3}$ at frequency of 200.7 GHz were also considered. The experimental conditions of the gyrotron at low and high voltages are simulated. The output power of 56 watts corresponds to the efficiency of 2 percent at low voltage operation and frequency of 394.6 GHz is expected.

Keywords Gyrotron · Continuous wave operation · Submillimeter wave ·
Dynamic nuclear polarization

1 Introduction

A gyortron is an important source of the short wavelength coherent radiation. High power gyrotrons in the millimeter wave range are developed worldwide for the electron cyclotron resonance heating (ECRH) of the plasma in nuclear fusion installations [1–3] and for technological applications [4]. An output power of 1 MW for a single tube and long pulse operation up to 1000 s have been achieved at frequency of 140 GHz [2]. In addition, high frequency medium power gyrotrons are of interest for plasma scattering measurements [5–7], electron spin resonance (ESR) experiments [8, 9], *etc.*

The Gyrotron is also an important source for performing dynamic nuclear polarization experiment at high field [10, 11] because of its capability to deliver microwave radiation with high stability in frequency and output power during long time periods as required for

L. Agusu (✉) · T. Idehara · I. Ogawa · T. Saito · T. Kanemaki
Research Center for Development of Far-Infrared Region, University of Fukui,
3-9-1 Bunkyo, Fukui 910-8507, Japan
e-mail: laagusu@fir.fukui-u.ac.jp

H. Takahashi · T. Fujiwara
Institute of Protein Research, Osaka University, 3-2 Yamadaoka, Osaka, Japan

the DNP-NMR experiment. In [10, 11] gyrotrons with frequencies of 140 GHz and 250 GHz were used. A significant enhancement of the NMR signal has been observed. Moreover, the operational characteristics of a 460 GHz gyrotron for NMR spectroscopy have also been demonstrated [12].

Operation at second harmonic of the cyclotron frequency allows higher frequencies to be obtained at lower magnetic fields. In other words, for a given frequency only half of the magnetic field is required in comparison with a gyrotron operating at the fundamental, for example, a low-power, continuous wave (CW), frequency tunable gyrotron at University of Sydney [13], and FU IVA gyrotron which has achieved frequency 889 GHz of frequency [14]. Recently, a 1 THz pulse gyrotron at University of Fukui has been tested [15]. It is well known that the harmonic interaction is inherently less efficient than the fundamental interaction due to elevated ohmic losses. It also suffers from additional complication due to mode competition and requires much higher beam currents in order to initiate oscillation. To a large extent, these difficulties can be reduced through an appropriate design.

In this work, we report the complete design and operating conditions of a 394.6 GHz gyrotron oscillator operating continuously at the second cyclotron harmonic for application in DNP-NMR spectroscopy. The presentation of this material is organized as follows. First, a brief overview of design considerations are presented, followed by mode selection analysis, and optimization of the gyrotron parameters which include performance of the gyrotron at high and low voltages operations and optimization of the gyrotron window. Finally, concluding remarks is given.

2 Gyrotron design considerations

The goal of this design is to successfully generate several tens of watts of CW power at the second harmonic and frequency of 394.6 GHz, a level sufficient to perform biological experiments using sensitivity-enhanced nuclear magnetic resonance (NMR) through dynamic nuclear polarization (DNP).

The design of the 394.6 GHz gyrotron oscillator is based on the previous 384 GHz gyrotron built at the Research Center for Development of Far-Infrared Region, University of Fukui (FIR Center FU) [16] which was used for plasma scattering measurements. This was also inspired by the successful experiments at a low power levels, CW submillimeter wave gyrotron at MIT [12] for application in NMR spectroscopy. The operating mode TE_{mn} with m<n at submillimeter regime is suitable for our existing electron optical system which can provide optimum beam radius for effective coupling with the electric field.

A schematic view of the 394.6 GHz gyrotron system is shown in Fig. 1. The axes of the gyrotron tube and electron beam lie along the bore of the 8 T superconducting magnet. There are two pumping bores. First is located near the electron gun to assure the vacuum condition inside the tube. Second is placed after the collector to pump out the out gassing from the electron collector as well as the resonator. In the continuous-wave (CW) operation, temperature of the cavity increases during the operation. In the experiment it has been observed such increase of temperature influence significantly the stability of the frequency and output power of CW gyrotron [17]. Therefore, the cooling system surrounding the cavity is absolutely necessary. The installed water jacket with a constant flow surrounds the whole gyrotron tube, including the electron collector, in order to maintain the tube temperature at a permissible level. On the collector, the energy of the spent electron beam is dissipated. The collector with inner diameter of 28 mm also serves as a microwave waveguide to the output window. The temperature of the collector increases to higher
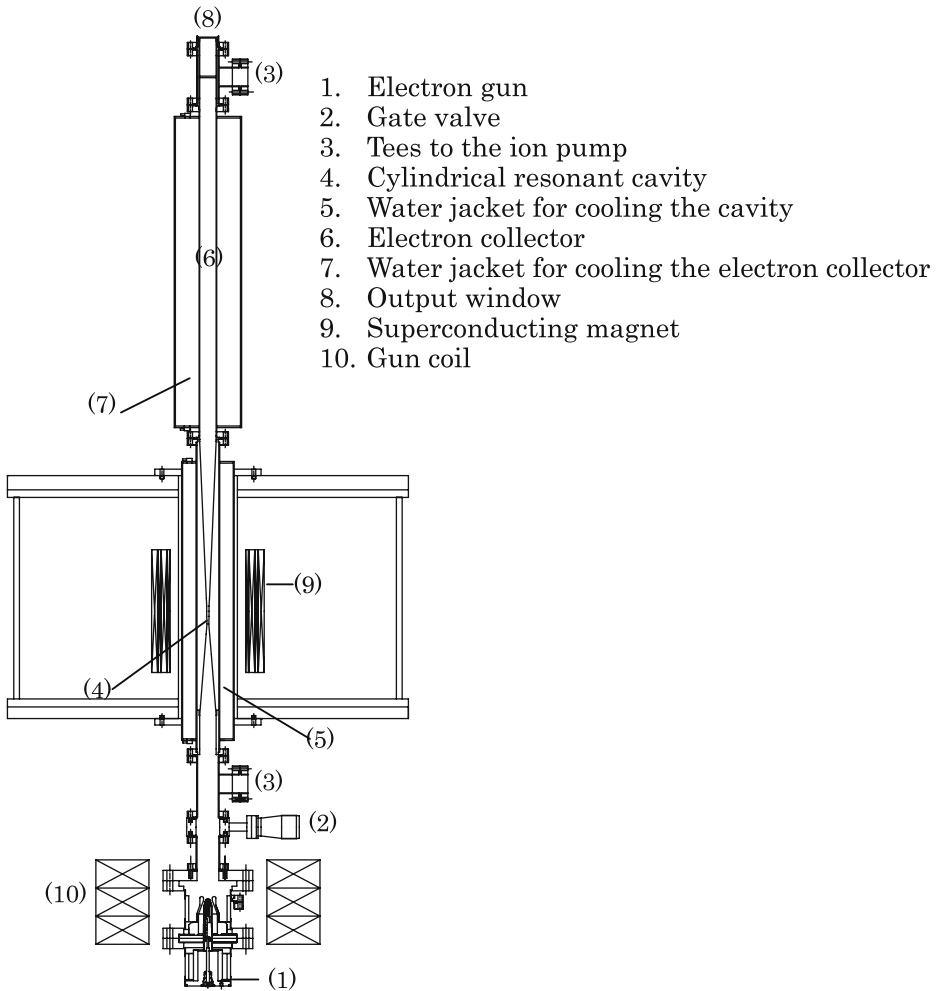
(8)

(3)

1. Electron gun
2. Gate valve
3. Tees to the ion pump
4. Cylindrical resonant cavity
5. Water jacket for cooling the cavity
6. Electron collector
7. Water jacket for cooling the electron collector
8. Output window
9. Superconducting magnet
10. Gun coil

(6)

(7)

(9)

(4)

(5)

(3)

(2)

(10)

(1)

Fig. 1 Cross-section of the cylindrical 394.6 GHz gyrotron. The gyrotron tube is approximately 1.7 m long and the magnet bore diameter is 10 cm.

values than temperature of the gyrotron tube. This is why; the diameter of the water jacket here is bigger than the diameter of water jacket of the cavity. The total length of tube including the collector is 1.7 m. Sets of two-axis horizontal adjustment stages are located upper and below the cryostat and are used to align the gyrotron tube with respect to the magnetic field of the superconducting magnet. The gyrotron tube is demountable which enables us to change some parts of it.

The electron optical system (EOS) is based on a triode magnetron injection gun (MIG) with accelerating voltage ranging from 10 to 25 kV. The cathode radius is 4.5 mm. In practice, the electron beam parameters such as the beam radius and velocity pitch factor can be experimentally tuned by a gun coils installed around the electron gun through changing the magnetic compression, the ratio of axial magnetic field at the cavity and cathode. The gun coils produce a maximum magnetic field of 0.13 T.

Initially, the design radius of the cavity optimized for operation on $TE_{2,6}$ mode at frequency of 394.6 GHz and $TE_{0,6}$ mode at a slightly higher frequency 396.69 GHz. Due to machining error however the cavity has been manufactured with a radius 2.372 mm, i.e. about 10–14 μm greater. Then the main operating mode with frequency close to 394.6 GHz shifted from $TE_{2,6}$ to $TE_{0,6}$ mode. The preliminary analysis shows that the optimized length of the cavity is 15 mm. Figure 2 shows the cross-section of a cylindrical cavity, consisting of a straight section of length 15 mm and circular cross-section of radius 2.372 mm joined to a linearly uptapered section with slope of 6.0° and a linearly downtapered section at the entrance with a slope angle of 2.5°. The axial profile of the designed mode, $TE_{0,6}$ is shown in the lower trace. The material of the cavity is copper.

3 Mode selection

It is well-known that the second harmonic modes are much more difficult to be excited than the fundamental one because of mode competition with fundamental mode. To successfully excite the second harmonic modes, the fundamental modes must be suppressed. The following ways are used to overcome this problem. A second harmonic cavity mode could be selected based on the fact that the fundamental mode spectrum is uneven. Clumping around certain frequency or mode indices (x_{mp}) tend to occur. One observes large gaps in the fundamental mode spectrum. Since a given mode is only excited over a limited region of magnetic field. Therefore, it is desirable to select the second harmonic mode that exists in a magnetic field corresponds to a gap in fundamental spectrum. Then the electron beam is placed in a position where the coupling to the fundamental mode is weak.

The frequency spacing between modes increases as the cavity radius is decreased. Thus, to improve operation at the second harmonic, a smaller cavity radius should be chosen in order to keep the modes farther apart and reduce competition between the fundamental and second harmonic.
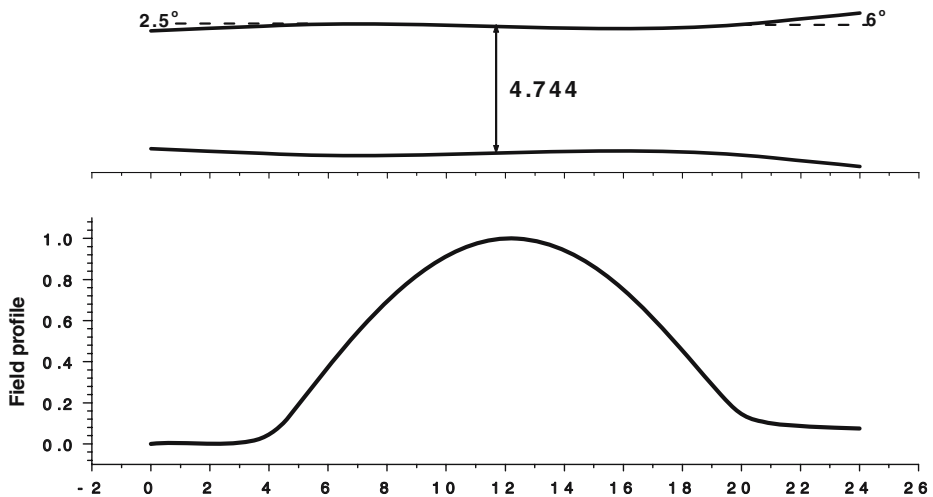

Fig. 2 Cross-section of a 394.6 GHz gyrotron cavity with the axial field profile for the second harmonic $TE_{0,6}$ mode. Input taper: $L_1=5$ mm, $\theta_1=2.5°$; Middle section $R=2.372$ mm, $L=15$ mm; output taper: $L_2=4$ mm, $\theta_2=6.0°$.

Figure 3 shows the beam-field coupling coefficient

$$J^2_{m\mp s}\left(x_{mp}R_b/R\right)\bigg/\left[\left(x^2_{mp}-m^2\right)J^2_m\left(x_{mp}\right)\right]$$

as a function of normalized radius R_b/R for the second harmonic modes $TE_{2,6}$, $TE_{0,6}$, and the fundamental mode $TE_{2,3}$. It is seen in Fig. 3 that if $R_b/R=0.68$ then $TE_{2,6}$ and $TE_{0,6}$ mode have high coupling to the electron beam, while coupling to the $TE_{2,3}$ is weak. As mentioned above that the desired frequency is 394.6 GHz then preferable cavity radius for these modes for operation at magnetic field $B<8$ T and voltage 25 kV is approximately 2.372 mm. In this case, the beam radius is 1.68 mm. The estimated magnetic field at the cathode using the relation

$$B_{cath}=\left(R_b/R_{cath}\right)^2 B$$

for $R_{cath}=4.5$ mm corresponds to magnetic field of 1.03 T. Unfortunately this field intensity can not be reached using our present magnets and power. In order to overcome this problem it has been decided to choose $R_b/R=0.16$ and $R_b/R=0.22$ for excitation of $TE_{0,6}$ and $TE_{2,6}$ modes, respectively, which are corresponding to the radii of 0.38 mm and 0.54 mm. The frequencies and quality factors for the $TE_{2,6}$, $TE_{0,6}$, and $TE_{2,3}$ modes are shown in Table 1.

The operation conditions of the gyrotron will be investigated for both high (∼25 kV) and low (∼7–14 kV) voltages regimes with the main operating modes $TE_{2,6}$ and $TE_{0,6}$ at the frequencies 392.614 GHz and 394.684 GHz, respectively. Figures 4, 5 show the starting currents of the cavity modes as a function of the magnetic field for two cases of high ($V_b=$
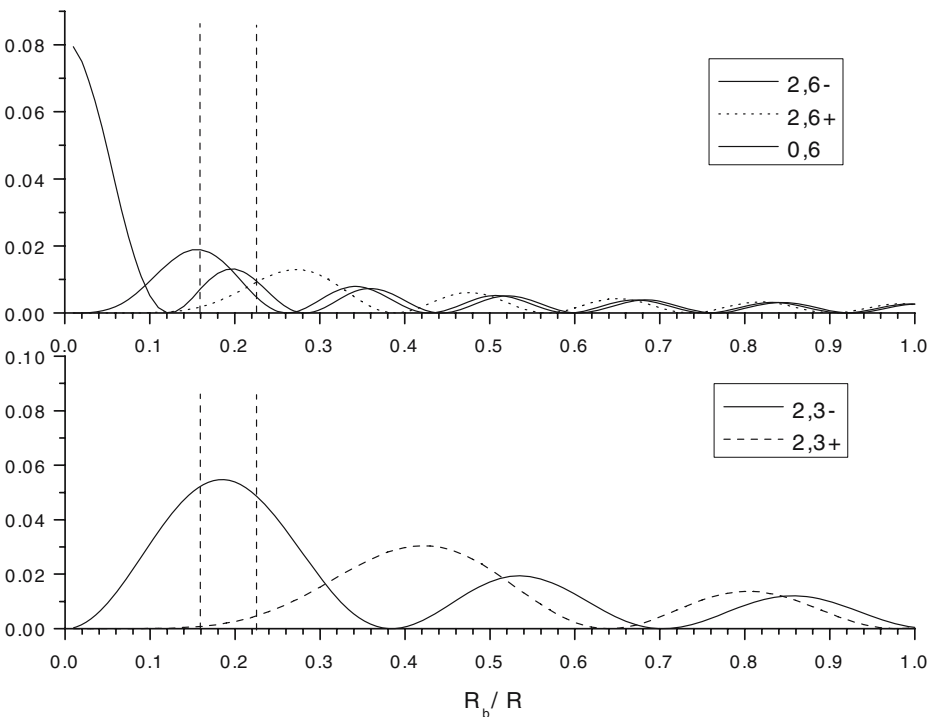

Fig. 3 Coupling coefficients as a function of normalized radius for the $TE_{2,6}$, $TE_{0,6}$ (upper trace) and $TE_{2,3}$ (lower trace) modes.

Table 1 List of the main cavity modes in area of interest.

TEmn Mode		Frequency (GHz)	Q	Harmonic number
m	n			
2	6	392.614	11179	2
0	6	394.684	11328	2
2	3	200.727	3367	1

25 kV) and low (V_b=14 kV) accelerating voltage. In each case two beam radii (0.54 mm and 0.38 mm) are considered. The radius of 0.54 mm is mainly for excitation of $TE_{2,6}$ mode at frequency of 392.6 GHz, and the radius of 0.38 mm is for excitation of $TE_{0,6}$ mode at frequency of 394.68 GHz. As an illustration how the beam radius could change the operation condition of those modes, in Fig. 4 as beam radius shift from 0.54 to 0.38 mm the minimum starting currents of $TE_{0,6}$ and $TE_{2,6}$ modes decreased from 0.293 to 0.065 A and from 0.183 to 0.237 A, respectively.

In addition, for high voltage operation the starting currents of those modes are overlapping due to broadening of the region of starting currents at high accelerating voltage. The mode competition between modes is more severe. Using the beam radius of 0.38 mm is absolutely important (see lower-half of Fig. 4). Moreover, operation at low voltage is more feasible for excitation of both $TE_{2,6}$ and $TE_{0,6}$ modes since their starting currents are well-separated from each other (see Fig. 5 with the voltage of 14 kV).
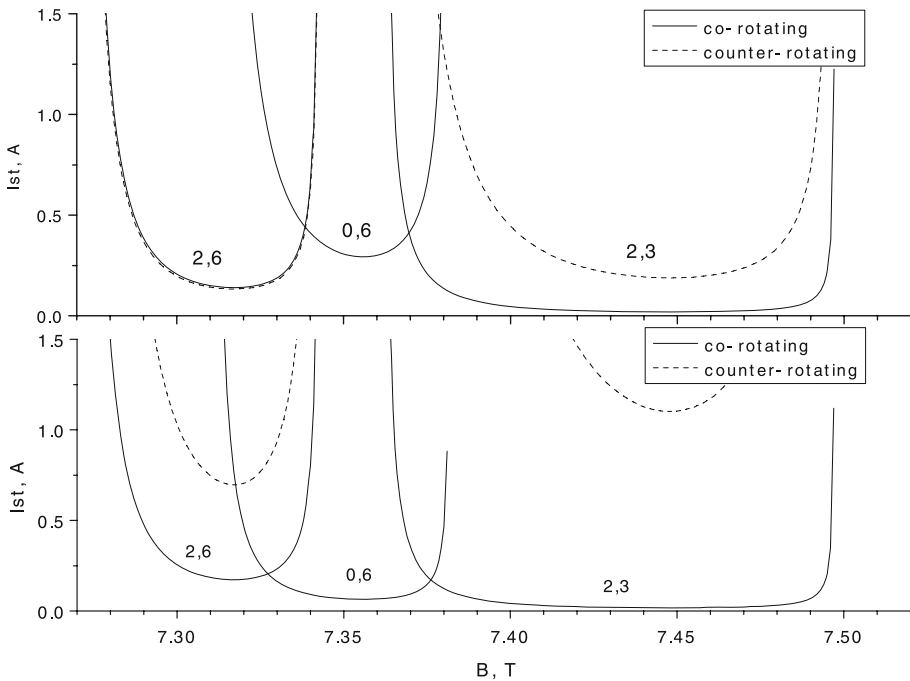

Fig. 4 Starting currents of the $TE_{2,6}$, $TE_{0,6}$ (second harmonic) and $TE_{2,3}$ (fundamental) modes for operation using beam voltage 25 kV and beam radii: 0.54 mm (upper trace) and 0.38 mm (lower trace).
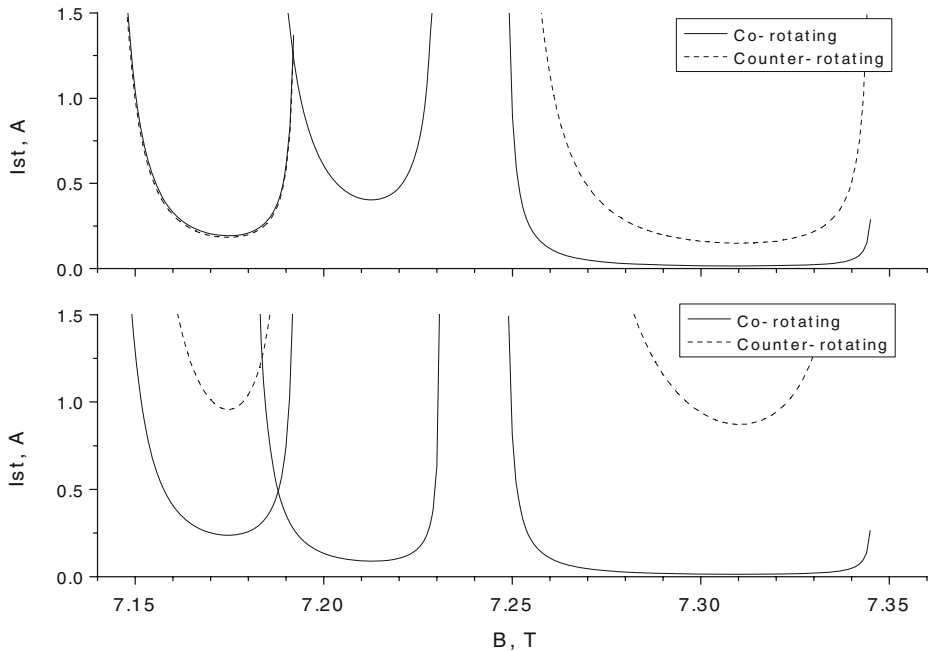
Fig. 5 Starting currents of the TE$_{2,6}$, TE$_{0,6}$ (second harmonic) and TE$_{2,3}$ (fundamental) modes for operation using the beam voltage 14 kV and beam radii: 0.54 mm (upper trace) and 0.38 mm (lower trace).

Figure 6 shows comparison result of the minimum starting currents of the TE$_{2,6}$, TE$_{0,6}$, and TE$_{2,3}$ modes, and their corresponding magnetic field as a function of beam voltage. Two cases of beam radii 0.54 mm and 0.35 mm are shown in upper and lower-traces of Fig. 6. It is illustrated in Fig. 6 that as the voltage decreases form 28 to 11 kV, the minimum starting current of TE$_{2,6}$ increases from 0.1 to 0.2 A for beam radius 0.54 mm (upper-curve), while the minimum starting current of TE$_{0,6}$ mode increases from 0.03 to 0.1 A for beam radius of 0.38 mm (lower-curves).

This simplified analysis based on the linear theory is followed by more detailed one that takes into account mode competition in the next section.

4 Optimization of the gyrotron parameters

Operation conditions and performance of the gyrotron with the desired frequency 394.6 GHz are simulated using multi-mode time-dependent code for mode competition calculation. The physical model of mode competition used here (based on the ref. [18]) has been described in [19]. Operation conditions both at high and low-voltages are described. The Ohmic losses are taken into account in the calculation. Some other effects such as velocity spread, spreading of the guiding centers, and mode conversion are not taken into account in the simulation code.

The mode competition calculations were performed to find the operating conditions of single mode excitation of TE$_{2,6}$ (f=392.641 GHz), TE$_{0,6}$ (f=396.69 GHz) at second harmonic and TE$_{2,3}$ (f=201.75 GHz) at the fundamental (see in Table 1). In the real experiment there are, at least, four parameters which can be varied: beam current, I_b,
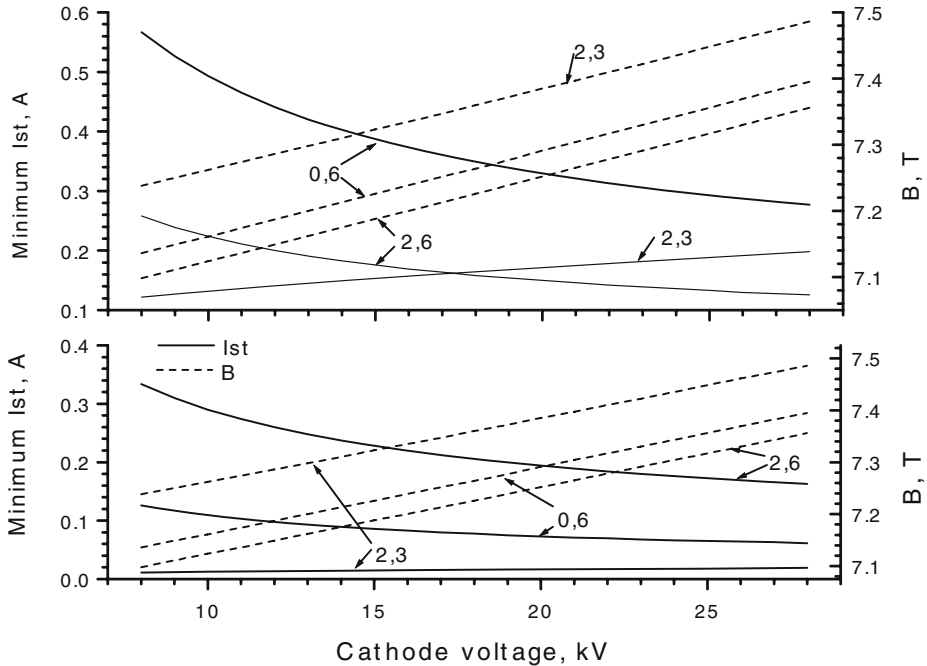
Fig. 6 The minimum starting currents of TE$_{2,6}$, TE$_{0,6}$, and TE$_{2,3}$ modes and their corresponding magnetic field as a function of beam voltage. Results with the beam radii 0.54 mm and 0.38 are shown in upper and lower-curves, respectively.

cathode voltage, Vc, current of superconducting magnet (corresponds to the field in cavity, B), and gun coil current (corresponds to the beam radius, r_b). Dependence of RF power of gyrotron on those operating parameters are investigated.

4.1 High voltage operation

Figures 7, 8 demonstrate performance of the gyrotron on the variation of the beam current and main magnetic field. In Fig. 7 the gyrotron performance by tuning the magnetic from 7.23 to 7.53 T is shown. The TE$_{2,6}$ and TE$_{0,6}$ modes at second harmonic and frequencies of 392.6 GHz and 394.68 GHz can be excited in single mode operation by adjusting the magnetic field. It is seen in Fig. 7 that for operation using beam voltage 25 kV the optimum magnetic fields for single mode excitation of TE$_{2,6}$, TE$_{0,6}$, and TE$_{2,3}$ are 7.32, 7.34, and 7.41 T, respectively.

It is well-known that often mode competition is more severe at higher beam current. In order to investigate the stability of modes as the beam current increases mode competition calculations are performed at a fixed magnetic field corresponds to the optimum magnetic fields for each cavity modes. Figure 8 compares the output power of TE$_{2,6}$ (B=7.32 T), TE$_{0,6}$ (B=7.34 T), and TE$_{2,6}$ (B=7.41 T) as the beam current increases. The output power plotted in Fig. 8 is only for single mode operation for each mode. We have investigated the current increase up to 0.6 A. The TE$_{2,6}$ (second harmonic) and TE$_{2,3}$ (fundamental) modes can be excited without competition up to the current of 0.6 A while TE$_{0,6}$ is excited in single mode operation only up to the beam current of 0.4 A.
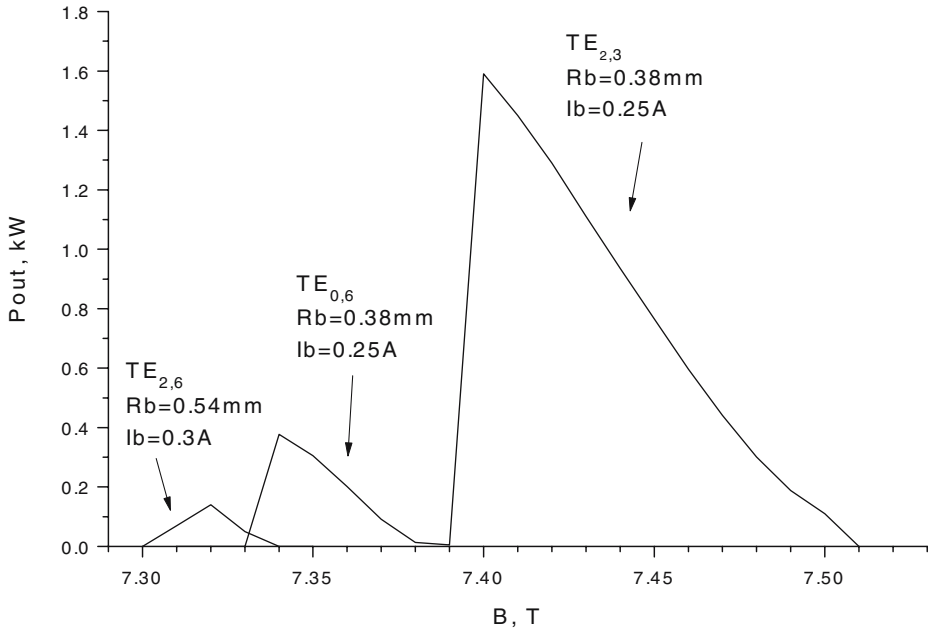
Fig. 7 The output power of $TE_{2,6}$, $TE_{0,6}$, and $TE_{2,3}$ at the voltage of 25 kV as a function of the magnetic field. Here, the $TE_{2,6}$ is exited using beam radius 0.54 mm and current of 0.3 A, while the $TE_{0,6}$ and $TE_{2,3}$ modes are exited for beam radius 0.38 mm and current of 0.25 A.
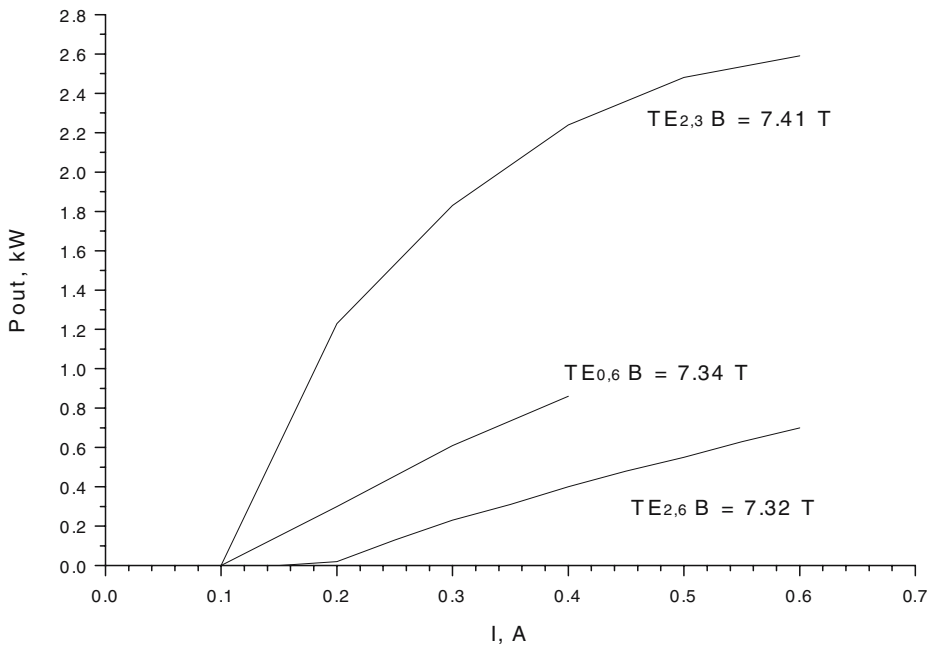

Fig. 8 Output power vs. beam current for $TE_{2,6}$ (B=7.32 T), $TE_{0,6}$ (B=7.34 T), and $TE_{2,3}$ (B=7.41 T) modes. Here, Vc=25 kV and α=1.6.

4.2 Low voltage operation

For a gyrotron applied in DNP-NMR spectroscopy that requires low power level (ten or several tens watts) in CW, the low voltage operation has more benefit in order to simplify the cooling system. Simulation results of low voltage operation of the gyrotron are presented. In all cases the cathode voltage is 13.7 kV.

The magnetic regimes of single mode operation of the $TE_{2,6}$, $TE_{0,6}$, and $T_{2,3}$ are identified. Figure 9 shows the output power as a function of the magnetic field. The optimum magnetic field of those modes are 7.17 T, 7.2 T, and 7.26 T respectively. Figure 10 shows the output power of $TE_{2,6}$ mode for two different magnetic fields (7.16 T and 7.17 T) as a function of beam current. Performance of $TE_{0,6}$ mode as the beam current increases is shown in Fig. 11. This mode can be exited even from the low current (0.15 A) if the magnetic field is adjusted to the value of 7.2 T.

4.3 Gyrotron window

The gyrotron window used in the initial experiment is made of a sapphire with a diameter and thickness 33 mm and 2.5 mm, respectively. This gyroron window, however, is more transparent for the frequency of 390 GHz than for the desired frequency 394.6 GHz. It is seen in Fig. 12 that at the frequency of 394.6 GHz, only 47 percent of power is transmitted where 99 percent of microwave power is transmitted at frequency of 370 GHz and other corresponding peak. Thus, all output power mentioned in Sections 4.1–4.2 has to be taken
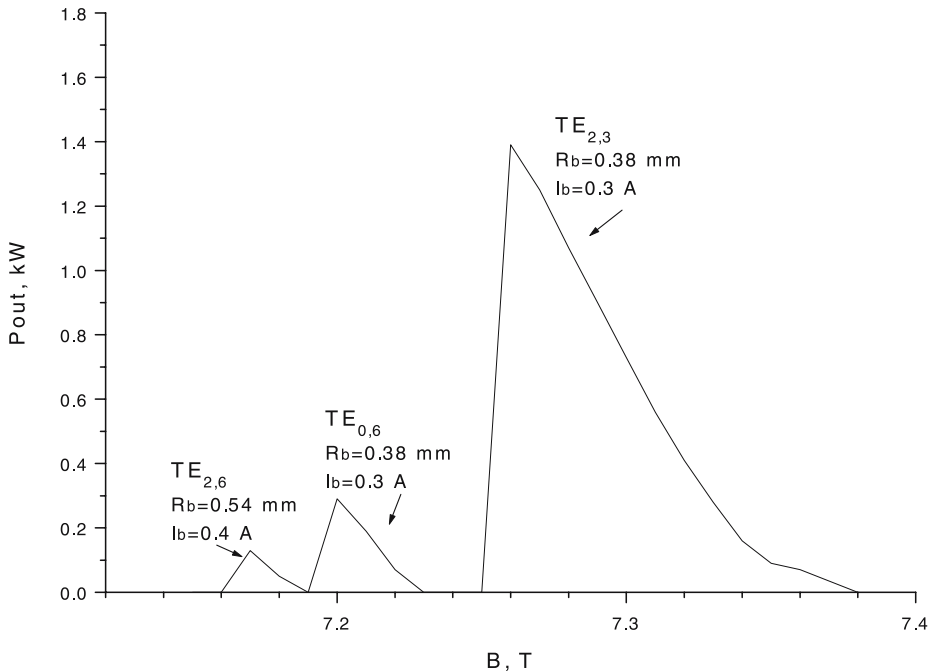

Fig. 9 The output power of $TE_{2,6}$, $TE_{0,6}$, and $TE_{2,3}$ at the voltage of 13.7 kV as a function of magnetic field. Here, the $TE_{2,6}$ is exited using beam radius 0.54 mm and current of 0.4 A, while the $TE_{0,6}$ and $TE_{2,3}$ modes are exited using beam radius 0.38 mm and current of 0.3 A.
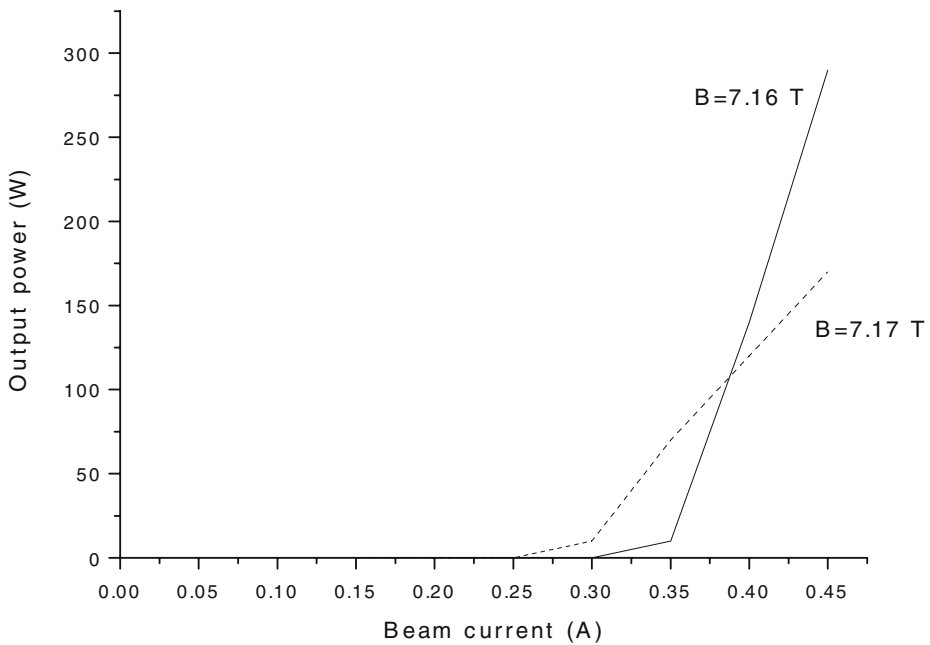
Fig. 10 Output power of excitation of $TE_{2,6}$ mode (beam radius of 0.54 mm) at frequency of 392.6 GHz, beam voltage of 13.7 kV and different magnetic fields (B=7.16 T and B=7.17 T) as a function of the beam current.

only 47, 99 and 44 percents of them for power excited by the $TE_{2,6}$, $TE_{0,6}$, and $TE_{2,3}$, respectively. Then by considering transmitted microwave power only 47 percent, the output power of $TE_{0,6}$ mode at 394.6 GHz and B=7.2 T (see Fig. 11) is approximately 56 watts corresponds to the efficiency of 2 percent when the beam voltage and current are 13.7 kV and 200 mA.

It is desirable to optimize the thickness of window in order to make it transparent for the frequency of 394.6 GHz. Figure 13 shows the transitivity of the optimized window with thickness of 2.71 mm.

Fig. 11 Output power of $TE_{0,6}$ mode (beam radius of 0.38 mm) at frequency of 394.68 GHz, voltage of 13.7 kV and different magnetic fields B=7.19, 7.20, and 7.22 T, as a function of the beam current.
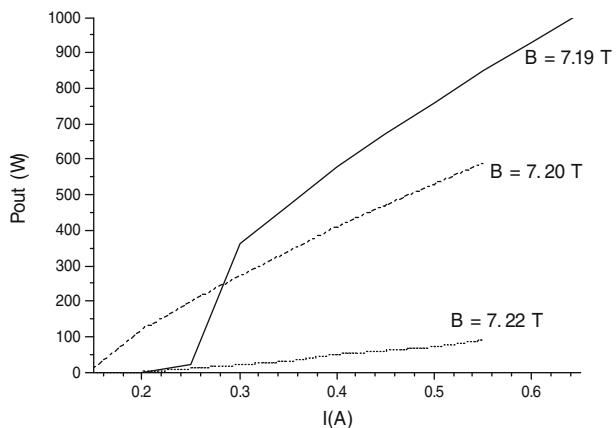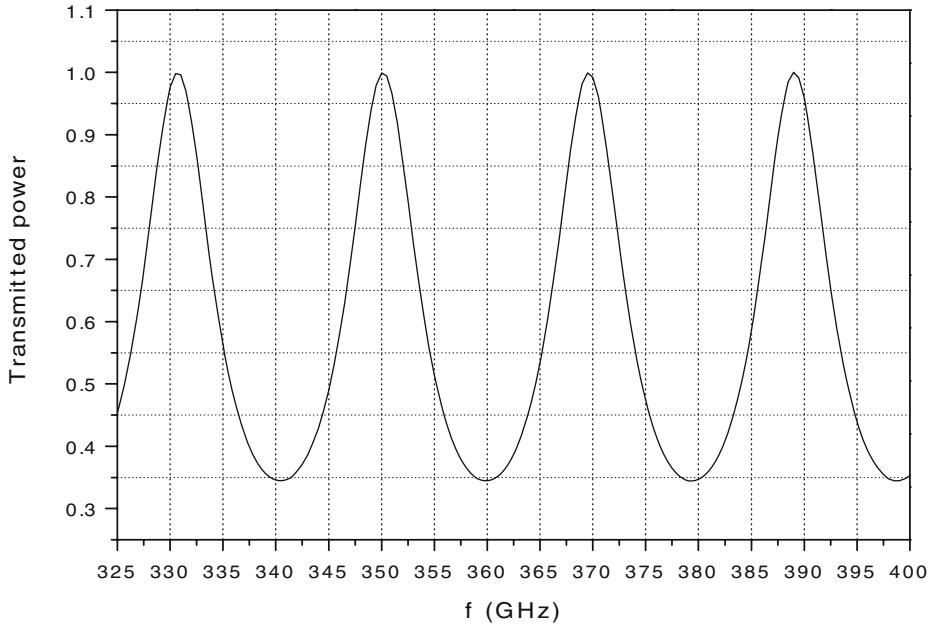
Fig. 12 Power transitivity of a sapphire windows versus frequency: ε_r=9.5, d=2.5 mm.

5 Conclusion

The gyrotron for sensitivity enhancement of NMR spectroscopy through the dynamic nuclear polarization has been designed. The gyrotron operates at the second harmonic and
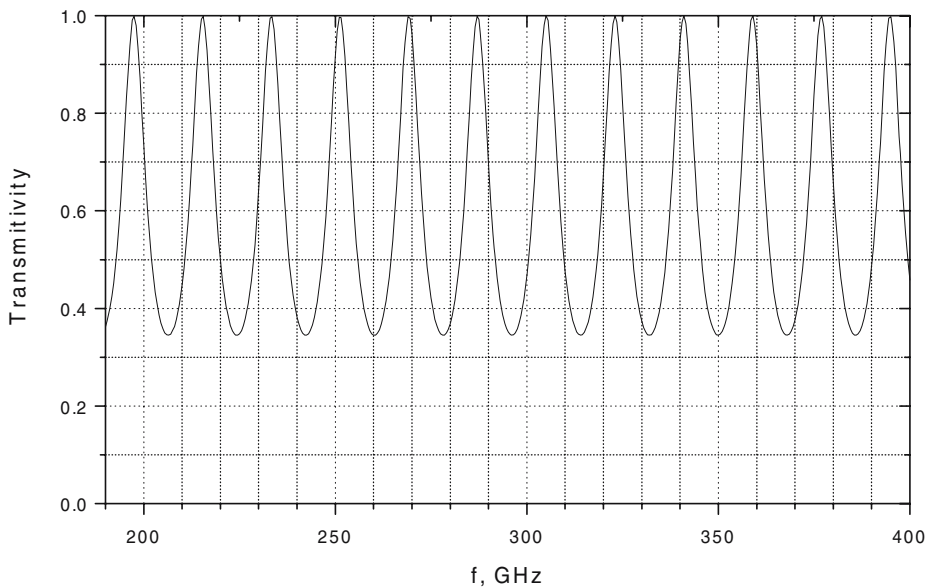

Fig. 13 Power transitivity of a new design sapphire windows versus frequency: ε_r=9.5, d=2.71 mm.

frequency of 394.6 GHz with the main operating mode $TE_{0,6}$. Operating conditions of other neighboring cavity modes such as $TE_{2,6}$ at frequency of 392.6 GHz and $TE_{2,3}$ at frequency of 200.7 GHz were also considered. The experimental conditions of the gyrotron at low and high voltages are simulated. The output power of 56 watts corresponds to efficiency of 2 percent at low voltage operation and frequency 394.6 GHz could be achieved.

References

1. M. Thumm, State-of-the-Art of High Power Gyro-Devices and Free Electron Masers Update 2005, Scientific Report FZKA 7198, Forschungszentrum Karlsruhe, Germany, February 2006.
2. V. Erckmann, G. Dammertz, D. Dorst, L. Empacher, W. Forster, G. Gantenbein, T. Geist, W. Kasparek, H. P. Laqua, G. A. Muller, M. Thumm, M. Weissgerber, and H. Wobig, ERCH and ECCD with high power gyrotrons at the stellaraors W7-AS and W7X, IEEE Trans. Plasma Sci. **27**, 538–546 (1999).
3. V. L. Granatstein, B. Levush, B. G. Danly, and R. K. Parker, A quarter century of gyrotron research and development, IEEE Trans. Plasma Sci. **25**, 1322–1335 (1997).
4. G. Link, L. Feher, M. Thumm, H.-J. Ritzhaupt-Kleissl, R. Bohme, and A. Weisenberger, Sintering of advanced ceramics using a 30-GHz, 10-kW, CW industrial gyrotron, IEEE Trans. Plasma Sci. **27**, 547–556 (1999).
5. I. Ogawa, K. Yoshisue, H. Ibe, T. Idehara, and K. Kawahata, Long-pulse operation of a submilimeter wave gyrotron and its application to plasma scattering measurement, Rev. Sci. Instrum. **65**, 1778–1789 (1994).
6. Y. Shimizu, S. Makino, K. Ichikawa, T. Idehara, and I. Ogawa, Development of submillimeter gyrotron for plasma diagnostic, Fusion Eng. Sci. **26**, 335–340 (1995).
7. T. Idehara, S. Mitsudo, M. Ui, I. Ogawa, M. Sato, and K. Kawahata, Development of frequency tunable gyrotrons in millimeter to submillimeter wave range for plasma diagnostics, J. Plasma Fusion Res. Series **3**, 407–410 (2000).
8. T. Tatsukawa, T. Maeda, H. Sasai, T. Idehara, M. Mekata, T. Saito, and T. Kanemaki, ESR spectroscopy with a wide frequency range using a gyrotron as a radiation power source, Int. J. Infrared Millim. Waves **16**, 293–305 (1995).
9. S. Mitsudo, Aripin, T. Matsuda, T. Kanemaki, and T. Idehara, High power, frequency tunable, submillimeter wave ESR device using a gyrotron as a radiation source, Int. J. Infrared Millim. Waves **21**, 661–676 (2000).
10. L. N. Becerra, G. J. Gerven, R. J. Temkin, D. J. Singel, and R. G. Griffin, Dynamic nuclear polarization with a cyclotron resonance maser at 5 T, Phys. Rev. Lett. **71**, 3561–3564 (1993).
11. V. S. Bajaj, C. T. Farrar, M. K. Hornstein, I. Mastovsky, J. Vieregg, J. Bryant, B. Elena, K. E. Kreischer, R. J. Temkin, and R. G. Griffin, Dynamic nuclear polarization at 9 T using a novel 250 GHz gyrotron microwave source, J. Magn. Reson. **160**, 85–90 (2003).
12. M. K. Hornstein, V. S. Bajaj, R. G. Griffin, and R. J. Temkin, Continuous-wave operation of a 460-GHz second harmonic gyrotron oscillator, IEEE Trans. Plasma Sci. **34**, 524–533 (2006).
13. G. F. Brand, Development and application of frequency tunable, submillimeter wave gyrotrons, **16**(5), 879–887 (1995).
14. T. Idehara, I. Ogawa, S. Mitsudo, M. Pereyaslavets, N. Nishida, and K. Yoshida, Development of frequency tunable, medium power gyrotrons (Gyrotron FU Series) as submillimeter wave radiation sources, IEEE Trans. Plasma Sci. **27**, 340–354 (1999).
15. T. Idehara, H. Tsuchiya, O. Watanabe, La Agusu, and S. Mitsudo, The first experiment of a THz gyrotron with a pulse magnet, Int. J. Infrared Millim. Waves **27**, 319 (2006).
16. T. Idehara, T. Tatsukawa, I. Ogawa, H. Tanabe, T. Mori, S. Wada, G. F. Brand, and M. H. Brennan, Development of a second cyclotron harmonic gyrotron operating at submillimeter wavelength, Phys. Fluids B **4**, 267–273 (1991).
17. T. Idehara, Y. Iwata, and I. Ogawa, Observation of frequency-domain shift in a submillimeter wave gyrotron, Int. J. Infrared Millim. Waves **24**, 119–128 (2003).
18. N. A. Zavolsky, G. S. Nusinovich, and A. B. Pavelyev, Stability of single mode oscillations and nonstationay processes in gyrotron with oversized low-quality resonators, in *Gyrotrons*, edited by A. V. Gaponov-Grekhov (Institute of Applied Physics, Academy of Sciences of the USSR, Gorky, 1989, pp. 84–112). Collection of scientific papers.
19. La Agusu, T. Idehara, H. Mori, T. Saito, I. Ogawa, and S. Mitsudo, Design of a CW THz gyrotron (Gyrotron FU CW III) using a 20 T superconducting magnet, Int. J. Infrared Millim. Waves **28**, 315–328 (2007).